MOEM

Modern Electronic Materials 4(2): 53–58
DOI 10.3897/j.moem.4.2.33839

Research Article

Supercontinuum generated high power highly nonlinear photonic crystal fiber for medical and optical communications applications

Feroza Begum[1], Hazwani Suhaimi[1], Norazanita Shamsuddin[1], Martin Geoffrey Blundell[1], Yoshinori Namihira[2]

1 Faculty of Integrated Technologies, Universiti Brunei Darussalam, Gadong BE 1410, Brunei Darussalam

2 Graduate School of Engineering and Science, University of the Ryukyus, Okinawa 903-0213, Japan

Corresponding author: *Feroza Begum* (feroza.begum@ubd.edu.bn)

Received 2 April 2017 ♦ **Accepted** 19 February 2018 ♦ **Published** 1 June 2018

Citation: Begum F, Suhaimi H, Shamsuddin N, Martin Blundell MG, Namihira Y (2018) Supercontinuum generated high power highly nonlinear photonic crystal fiber for medical and optical communications applications. Modern Electronic Materials 4(2): 53–58. https://doi.org/10.3897/j.moem.4.2.33839

Abstract

This paper investigates a supercontinuum generated high power highly nonlinear photonic crystal fiber for medical and optical communication applications. The full vector finite difference method with perfectly matched layer is used as an analysis tool. Numerical simulation results show that it is possible to achieve high nonlinear coefficient, near zero ultra-flattened dispersion, low confinement loss and supercontinuum spectrum with high power. Moreover, numerical results show that short length of the proposed photonic crystal fiber is achieved. The numerical simulation results of supercontinuum generation is conducted by solving the generalized nonlinear Schrödinger equation with the split-step Fourier method. It is observed adequate supercontinuum spectrum that broaden from 960 to 1870 nm by considering center wavelengths of 1.06, 1.31, and 1.55 μm into silica based index guiding photonic crystal fiber. This simulation results prove that the proposed design of a highly nonlinear photonic crystal fiber is a great solution for broad supercontinuum generation with high power.

Keywords

photonic crystal fiber, nonlinear coefficient, confinement loss, supercontinuum spectruum

1. Introduction

Photonic crystal fibers **(PCFs)** have attracted a lot of interest of researchers because of their many unique properties which are not found in conventional optical fibers [1, 2]. PCFs arrays of air hole run along the length of fiber. The shape, size, number and distribution of air holes contribute to achieve many unique properties. The core of this particular fiber is made of single material such as silica and can either be solid or hollow. The PCF is divided into two different fibers: one is index guiding photonic crystal fiber and other one is photonic band gap fiber. In index guiding PCF light is guided by the total internal reflection between the solid core and multiple air holes cladding. Photonic band gaps cause the periodicity of the crystal induced a gap in its band structure. No electromagnetic modes are allowed to have frequency in the gap. They have shown great properties in nonlinear fiber optics such as supercontinuum **(SC)** generation [3] and in many other no-

vel fiber devices [4]. Control of chromatic dispersion, simultaneously keeping the confinement loss to a level below the Rayleigh scattering limit is very important for communication systems, both in the linear and the nonlinear regimes, and for any optical systems that support ultrashort soliton pulse propagation. In all cases, an almost flattened fiber dispersion and low confinement loss behavior becomes a crucial issue.

To date, different supercontinuum generated highly nonlinear photonic crystal fibers (HN-PCFs) have been suggested for optical communications and medical applications [5–16]. The reported HN-PCFs [5] have nonlinear coefficients of about 30 $W^{-1}km^{-1}$ at 1.55 μm wavelength, although there is increased design complexity, because four to five different air-hole diameters are needed. The wavelength near 1.0 and 1.3 μm are especially attractive in ophthalmology and dentistry, respectively because they offer optical coherence tomography **(OCT)** imaging with minimum dispersion, deeper penetration and improved sensitivity. Superluminescent diodes **(SLDs)** with 20 to 80 nm optical bandwidth, yield low output power 2 to 15 mW [6]. Femtosecond laser with narrow band SC spectrum and low output power were demonstrated experimentally or numerically by several groups [7–16]. Neodymium-doped $Y_3Al_5O_{12}$-crystals **(Nd:YAG)** were investigated at around 1.0 μm center wavelength [7]. The spectrum bandwidth was approximately 0.2 nm and output power 1.3 W. Generation a SC spectrum pumped with 200 fs Yb-doped fiber laser at a central wavelength of 1.07 μm is reported [8]. As a result, 11 nm spectrum full width half maximum **(FWHM)** and 800 mW output power was obtained. Ultrahigh resolution OCT is demonstrated at 1.3 μm center wavelength using continuum generation in a single photonic crystal fiber with a 85 fs pulse train from a compact Nd:Glass oscillator [9]. As a result, 156 nm FWHM bandwidth spectrum and 48 mW output power are reported. A Ge-doped PCF picosecond pulse laser was investigated at 1.31 μm center wavelength [10]. The acquired FWHM spectrum of 75 nm. Based on the use of ytterbium-doped photonic crystal fiber, a 75 mW output power SC was generated from a 150 mW input signal wave at 1.064 μm [11]. The broadband spectrum in IR region was generated with 100 W pump peak power at 1.55 μm using a CS_2 core photonic crystal fiber [12]. SC sources based on a GeO_2 doped core fiber which was being pumped by a broadband four stage Er-Yb doped fiber [13]. A highest output power of 13.17 W was obtained after applying 34 W input pump power at around 1.0 μm wavelength. The generation of an ultra-broadband SC in silica PCF with As_2S_3 chalcogenide glass doped core was presented at wavelengths of 1.55 μm and 1.30 μm [14]. Femtosecond laser source with 3 kW peak power was used for the SC generation. HN-PCF was presented in OCT and telecommunication bands that produced supercontinuum spectra using picosecond pulses [15]. The maximum launched input peak powers of the presented HN-PCFs were 50.0 W, 14.0 W and 45.0 W at center wavelengths of 1.06 μm, 1.31 μm, and 1.55 μm, respectively. F. Begum et. al., explored the possibility of generating supercontinuum spectrum by using pico-second pulses in silicon dioxide core HN-PCF for ultrahigh-resolution OCT and optical transmission systems [16]. The input power of the incident pulse were 43.0 W, 8.0 W and 40.0 W, at center wavelength of 1.06 μm, 1.31 μm and 1.55 μm, respectively. It should be noted that SLDs still have suffered with low output power and narrow spectral bandwidth. On the other hand, femtosecond pulse laser-based SC sources possess a notable drawback of high implementation cost. Therefore, low cost picosecond pulse laser source which provide ultrabroadband light source with high power is a crucial issue for the practical implementation of high performance OCT.

In this paper, picosecond pulse based SC generated high power HN-PCF structure with near zero ultra-flattened dispersion, low confinement loss are proposed for the medical and optical communication applications. Numerical simulation results show that the proposed seven-ring HN-PCF having high nonlinear coefficients of about 106 $W^{-1}km^{-1}$ at center wavelength 1.06 μm, 74 $W^{-1}km^{-1}$ at center wavelength 1.30 μm and 53 $W^{-1}km^{-1}$ at center wavelength 1.55 μm. Moreover, it has been found that the proposed SC generated HN-PCF can exhibits very low confinement loss of less than 10^{-6} dB/km in the 1.0 to 1.60 μm wavelength range and near zero ultra-flattened chromatic dispersion in the targeted wavelength range. Furthermore, a high input power SC spectrum was obtained at center wavelengths 1.06, 1.30 and 1.55 μm. Additionally, it is also represent the fiber length of 1.0 m in all of the center wavelength for the proposed HN-PCF.

2. Method for simulation

A simulation tool using finite difference method with anisotropic perfectly matched layer boundary condition for designing and simulating proposed HN-PCF [17–19]. We have determined the real part and the imaginary parts of effective mode index after simulation which is then used to calculate confinement loss and chromatic dispersion. Using the real part of the effective mode index we have calculated the chromatic dispersion and the imaginary part of the effective mode index was used to calculate the confinement loss of HN-PCF. The effective area can be calculated directly using the software by solving the appropriate equation. The material dispersion is taken into account during the calculation by the Sellemier formula. The chromatic dispersion, dispersion slope, confinement loss and effective area are calculated by the following equations [17–19].

$$D = -\frac{\lambda}{c}\frac{\mathrm{d}^2\,\mathrm{Re}\left(n_{\mathrm{eff}}\right)}{\mathrm{d}\lambda^2} \tag{1}$$

$$D_S = \frac{\partial D(\lambda)}{\partial \lambda} \tag{2}$$

$$L_C = 8.686 k_0 \mathrm{Im}(n_{\mathrm{eff}}) \quad (3)$$

$$A_{\mathrm{eff}} = \frac{2\pi\left(\int_0^{\infty}\left|E_a(r)^2\right| r\mathrm{d}r\right)^2}{\int_0^{\infty}\left|E_a(r)\right|^4 r\mathrm{d}r} \quad (4)$$

where λ is the wavelength, n_{eff} is the complex refractive index, $\mathrm{Re}(n_{\mathrm{eff}})$ is the real part of the complex refractive index, $\mathrm{Im}(n_{\mathrm{eff}})$ is the imaginary part of the complex refractive index, k_0 is the free space wave number, $E_a(r)$ is the field amplitude at radius r.

Sellmeier equation is an empirical relationship between refractive index and wavelength for particular transparent and non-transparent medium. This equation is used to determine the dispersion of light. So the equation is define as

$$n_{\mathrm{eff}}^2 = 1 + \frac{B_1\lambda^2}{\lambda^2 + C_1} + \frac{B_2\lambda^2}{\lambda^2 + C_2} + \frac{B_3\lambda^2}{\lambda^2 + C_3} \quad (5)$$

where $B_{1,2,3}$ and $C_{1,2,3}$ are coefficients. The coefficients and values of Sellmeier equations are shown in Table 1 [17–19].

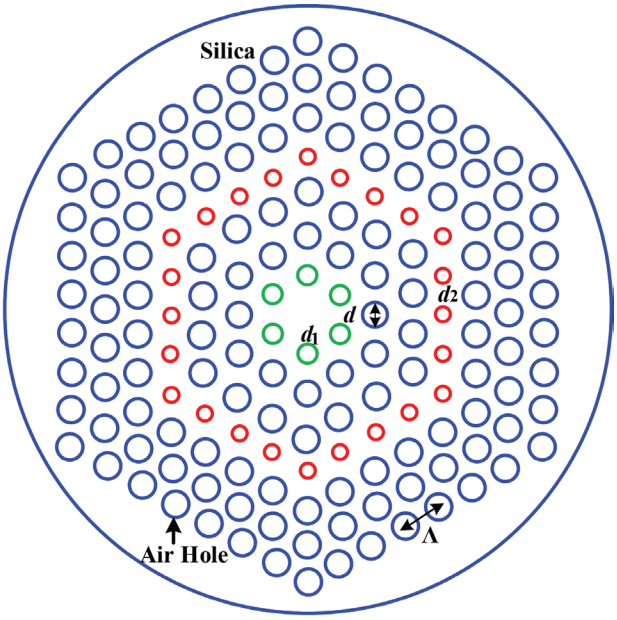

Figure 1. Proposed SC generated HN-PCF with seven rings of air hole with three different diameters d_1, d_2, d, and pitch Λ.

Table 1. Coefficients and values of Sellmeier equation.

Coefficient	Value
B_1	0.6961663
B_2	0.4079426
B_3	0.8974794
C_1	$0.0684043 \cdot 10^{-6}$
C_2	$0.1162414 \cdot 10^{-6}$
C_3	$9.896161 \cdot 10^{-6}$

Since PCFs can confine high intensity light, it is expected that PCFs would have high nonlinearity. Nonlinear coefficient γ can be calculated [20] as:

$$\gamma = \frac{2\pi n_2}{\lambda A_{\mathrm{eff}}} \quad (6)$$

Where n_2 is the non-linear refractive index.

3. Research model

Fig. 1 shows the geometry of the proposed SC generated high power HN-PCF structure. It consists of seven rings with three different types of air hole. The first ring air hole has diameter of d_1, the fourth ring air hole diameters of d_2 whilst the rest of the rings air hole have diameters of d. The distance between centers of neighboring air holes (i.e. its pitch) is kept at Λ. The host material is made up from regular silica. Designing HN-PCF to control dispersion using a conventional PCF structure is difficult: therefore, the first and fifth rings air hole diameter of the proposed HN-PCF are scaled downed to obtain the desired dispersion characteristics. The dimensions of the other rings are retained sufficiently large for better field confinement. To demonstrate the resultant characteristics of the proposed design, chromatic dispersion, low confinement loss, effective area and spectrum intensity should be analyzed for the optical communication and medical applications.

4. Results and discussion

A. Effective area and nonlinear coefficient

Figures 2 (a) and (b) represent the wavelength response of the effective area and nonlinear coefficient, respectively of the proposed SC generated high power HN-PCF. The parameters are pitch Λ = 0.87 μm, the first ring air hole diameter d_1 = 0.36 μm, the fourth ring air hole diameter d_2 = 0.31 μm, rest of the rings air hole diameter d = 0.80 μm. It is seen from Fig. 2(a) that the effective area is found 1.73 μm^2 at 1.06 μm, 2.02 μm^2 at 1.3 μm and 2.36 μm^2 at 1.55 μm which is smaller compared to that of conventional fibers (about 86 μm^2 at 1.55 μm wavelength). The corresponding nonlinear coefficients are more than 106 $[Wkm]^{-1}$ at 1.06 μm, 74 $[Wkm]^{-1}$ at 1.30 μm and 53 $[Wkm]^{-1}$ at 1.55 μm which is shown in Fig. 2(b).

B. Chromatic dispersion and chromatic dispersion slope

Figures 3 (a) and (b) show the wavelength response of chromatic dispersion and chromatic dispersion slope, respectively of the proposed SC generated high power HN-PCF. The parameters are pitch Λ = 0.87 μm, diameter of the first ring air hole d_1 = 0.36 μm, diameter of the fourth ring air hole d_2 = 0.31 μm, and the rest of the rings air

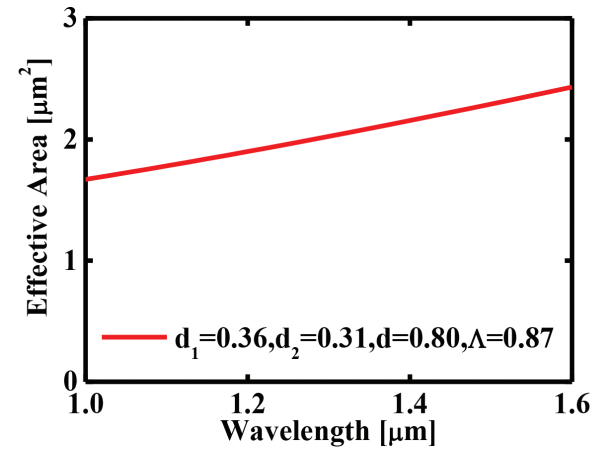

(a)

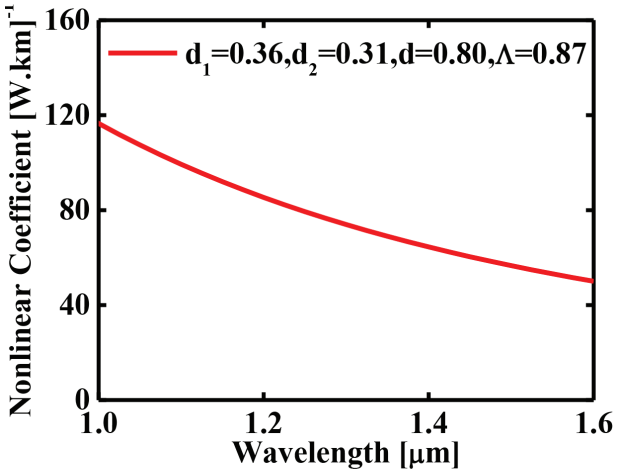

(b)

Figure 2. Wavelength dependence (a) effective area and (b) nonlinear coefficient for Λ = 0.87 μm, d_1 = 0.36 μm, d_2 = 0.31 μm and d = 0.80 μm of the proposed supercontinuum generated high power HN-PCF.

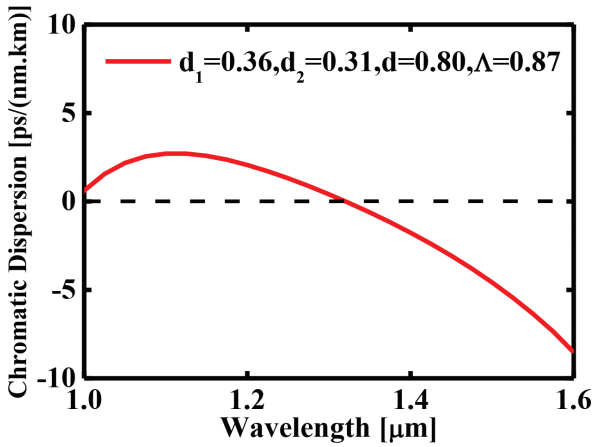

(a)

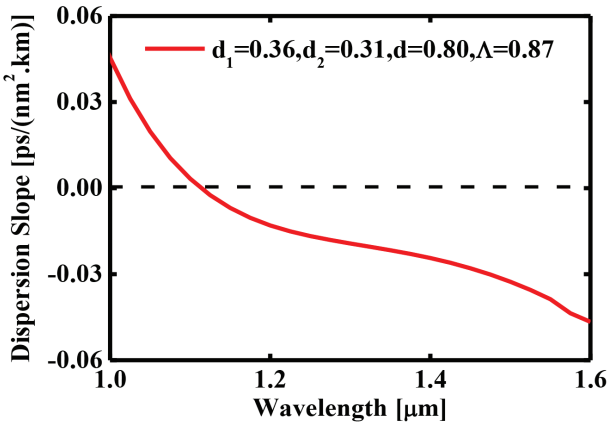

(b)

Figure 3. Wavelength dependence (a) chromatic dispersion and (b) chromatic dispersion slop for Λ = 0.87 μm, d_1 = 0.36 μm, d_2 = 0.31 μm and d = 0.80 μm of the proposed supercontinuum generated high power HN-PCF.

hole diameter d = 0.80 μm. It is seen that the real part of effective mode index has an effect on the chromatic dispersion. It is found that the wavelength range for which the proposed SC generated high power HN-PCF owning ultra-flattened chromatic dispersion ±8.5 ps/(nm.km) is from 1.0 μm to 1.60 μm. The chromatic dispersion slope is varied between ±0.04 ps/(nm².km) from 1.0 μm to 1.60 μm which is very small. This small dispersion slope which will offer the possibility of smaller pulse broadening for the wide bandwidth ranges.

C. Confinement loss

Figure 4 reveals the wavelength response of the confinement loss of the proposed SC generated high power HN-PCF. From Fig. 4, it is seen that the confinement loss is less than 10^{-6} dB/km in the entire wavelength range for the parameters Λ = 0.87 μm, d_1 = 0.36 μm, d_2 = 0.31 μm and d = 0.80 μm. This confinement loss is lower than the conventional optical fiber which is 0.2 dB/km at 1.55 μm wavelength.

D. Supercontinuum spectrum at 1.06 μm, 1.3 μm and 1.55 μm

Figures 5 (a), (b) and (c) show the wavelength response SC spectrum intensity of the proposed SC generated high power HN-PCF for the parameters Λ = 0.87 мм, d_1 = 0.36 мм, d_2 = 0.31 мм and d = 0.80 мм at wavelengths of 1.06 μm, 1.30 μm and 1.55 μm, respectively. The nonlinear Schrödinger equation (NLSE) is used for numerical calculation of SC spectrum [20]. The NLSE is solved by split-step Fourier method. SC generation in the proposed SC generated high power HN-PCF is numerically calculated at 1.06 μm, 1.30 μm and 1.55 μm center wavelengths which is shown in Fig. 5 (a), (b) and (c), respectively. In Fig. 5, consider the propagation of the sech² waveform with the full width at half maximum (FWHM), T_{FWHM} of 2.5 ps and Raman scattering para-

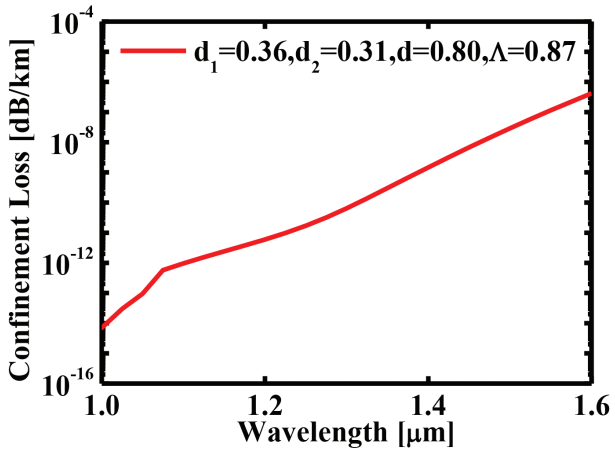

Figure 4. Wavelength dependence confinement loss for $\Lambda = 0.87$ μm, $d_1 = 0.36$ μm, $d_2 = 0.31$ μm and $d = 0.80$ μm of the proposed supercontinuum generated high power HN-PCF.

meter T_R of 3.0 fs through the proposed SC generated high power HN-PCF. The propagation constant around the carrier frequency β_2 and β_3 used in the calculation for Fig. 5 are shown in Table 2 at the center wavelengths of λ_c = 1.06 μm, λ_c = 1.30 μm and λ_c = 1.55 μm. From Fig. 5(a), it can be seen that the acquired spectrum range is from about 942 nm to 1210 nm at 1.06 μm center wavelength. The obtained range of spectrum is about 1128 nm to 1534 nm at 1.30 μm center wavelength which is shown in Fig. 5(b). Moreover, from Fig. 5(c), it can be seen that the acquired spectrum range is from about 1312 nm to 1895 nm at 1.55 μm center wavelength. After numerical simulation, the incident pulse input power P_{in} and fiber length L_F are obtained which is shown in Table 1. The achieved input powers are 2.9 kW at 1.06 μm center wavelength, 4.1 kW at 1.30 μm center wavelength and 5.5 kW at 1.55 μm center wavelength. The acquired fiber length L_F is 1 m in all the center wavelengths. These P_{in} values are higher and L_F values are lower than those of reported light sources [5–16].

5. Conclusion

In this research, a supercontinuum generated high power HN-PCF with seven rings of air hole was investigated. High nonlinear coefficients of 106 $[Wkm]^{-1}$, 74 $[Wkm]^{-1}$ and 53 $[Wkm]^{-1}$ with ultra-flattened chromatic dispersion of ±8.5 ps/(nm.km) in a wavelength range of 1.0 μm to 1.60 μm and low confinement loss of less than 10^{-6} dB/km in expected wavelength range was achieved. Moreover, it has been observed that this proposed SC generated high power HN-PCF could generate broad SC spectrum, and high powers of 2.9 kW, 4.1 kW and 5.5 kW at center wavelengths 1.06 μm, 1.30 μm and 1.55 μm, respectively were achieved. The proposed SC generated high power HN-PCF may be suitable for optical communications, optical parametric amplification, all-optical signal processing and supercontinum spectrum generation.

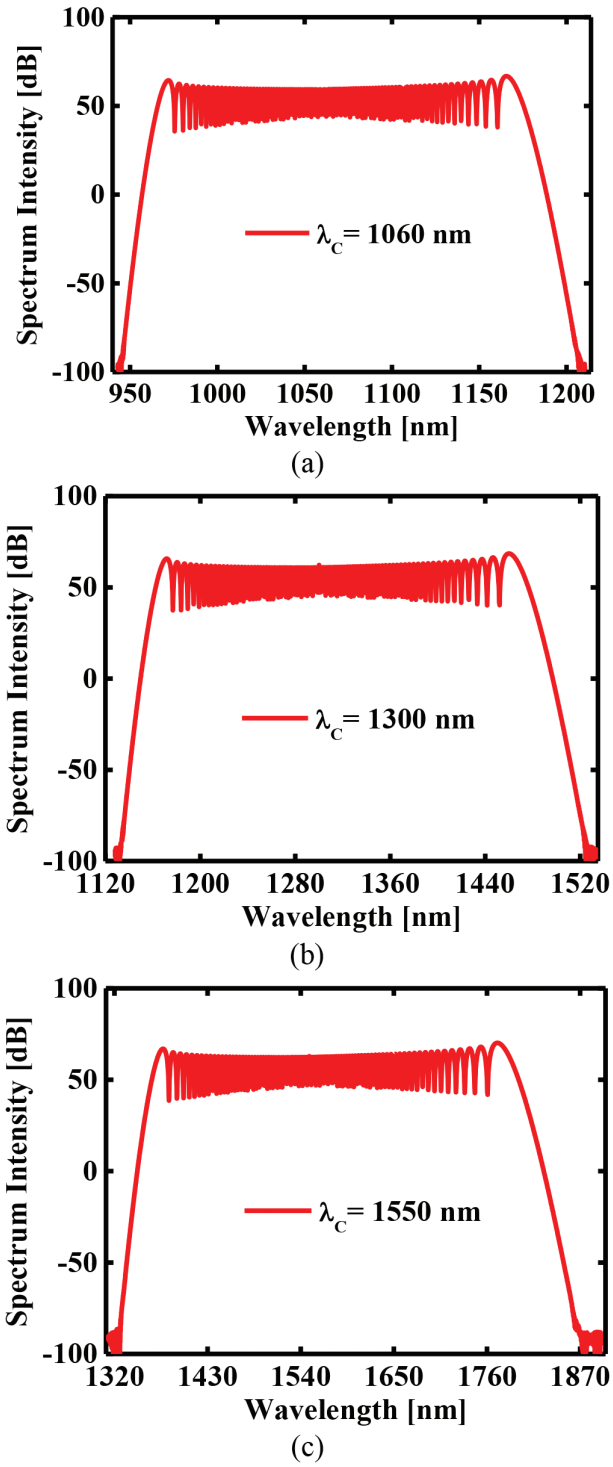

Figure 5. Spectrum intensity of the proposed SC generated high power HN-PCF at the center wavelengths (a) 1.06 μm, (b) 1.30 μm and (c) 1.55 μm.

Table 2. Fiber parameters.

Parameters	λ_c=1.06 [μm]	λ_c=1.30 [μm]	λ_c=1.55 [μm]
β_2 [ps^2/km]	1.013	1.524	2.166
β_3 [ps^3/km	0.014	0.004	0.013
P_{in} [kW]	2.9	4.1	5.5
L_F [m]	1.0	1.0	1.0

References

1. Joannopoulos J.D., Johnson S.G., Winn J.N., Meade R.D. Photonic Crystals Molding the Flow of Light. Princeton (USA): Princeton University Press, 2008.
2. Senior J.M. Optical Fiber Communications. Pearson Education Limited (UK), 2009.
3. Ranka J.K., Windeler R.S., Stentz A.J. Visible continuum generation in air silica microstructure optical fibers with anomalous dispersion at 800 nm. *Opt. Lett.*, 2000; 25(1): 25–27. https://doi.org/10.1364/OL.25.000025
4. Eggleton B.J., Kerbage C., Westbrook P.S., Windeler R.S., Hale A., Microstructured optical fiber devices. *Opt. Express*, 2001; 9(13): 698–713. https://doi.org/10.1364/OE.9.000698
5. Saitoh K., Koshiba M. Highly nonlinear dispersion-flattened photonic crystal fibers for supercontinuum generation in a telecommunication window. *Opt. Express*, 2004; 12(10): 2027–2032. https://doi.org/10.1364/OPEX.12.002027
6. Shibata H., Ozaki N., Yasuda T., Ohkouchi S., Ikeda N., Ohsato H., Watanabe E., Sugimoto Y., Furuki K., Miyaji K., Hogg R.A. Imaging of spectral-domain optical coherence tomography using a superluminescent diode based on InAs quantum dots emitting broadband spectrum with Gaussian-like shape. *Jpn. J. Appl. Phys.*, 2015; 54(4S): 04DG07-1-04DG07-5. https://doi.org/10.7567/JJAP.54.04DG07
7. Calmano T., Siebenmorgen J., Hellmig O., Petermann K., Huber G. Nd:YAG waveguide laser with 1.3 W output power, fabricated by direct femtosecond laser writing. *Appl. Phys. B*, 2010; 100(1): 131–135. https://doi.org/10.1007/s00340-010-3929-6
8. Zaytsev A., Lin C.-H., You Y.-J., Chung C.-C., Wang C.-L., Pan C.-L., Supercontinuum generation by noise-like pulses transmitted through normally dispersive standard single-mode fibers. *Opt. Express*, 2013; 21(13): 16056–16062. https://doi.org/10.1364/OE.21.016056
9. Aguirre A.D., Nishizawa N., Fujimoto J.G., Seitz W., Lederer M., Kopf D., Continuum generation in a novel photonic crystal fiber for ultrahigh resolution optical coherence tomography at 800 nm and 1300 nm. *Opt. Express*, 2006; 14(3): 1145–1160. https://doi.org/10.1364/OE.14.001145
10. Namihira Y., Hossain M.A., Koga T., Islam M.A., Razzak S.M.A., Kaijage S.F., Hirako Y., Higa H. Design of highly nonlinear dispersion flattened hexagonal photonic crystal fibers for dental optical coherence tomography applications. *Opt. Rev.*, 2012; 19(2): 78–81. https://doi.org/10.1007/s10043-012-0016-8
11. Louot C., Shalaby B.M., Capitaine E., Hilaire S., Leproux P., Pagnoux D., Couderc V. Supercontinuum generation in an ytterbium-doped photonic crystal fiber for CARS spectroscopy. *IEEE Photonics Technol. Lett.*, 2016; 28(19): 2011–2014. https://doi.org/10.1109/LPT.2016.2578721
12. Raj G.J., Raja R.V.J., Nagarajan N., Ramanathan G., Tunable broadband spectrum under the influence of temperature in IR region using CS_2 core photonic crystal fiber. *J. Lightwave Technol.*, 2016; 34(15): 3503–3509. https://doi.org/10.1109/JLT.2016.2571119
13. Jain D., Sidharthan R., Moselund P.M., Yoo S., Ho D., Bang O., Record power, ultra-broadband supercontinuum source based on highly GeO_2 doped silica fiber. *Opt. Express*, 2016; 24(23): 26667–26677. https://doi.org/10.1364/OE.24.026667
14. Ali R.A.H., Hameed M.F.O., Obayya S.S.A. Ultrabroadband supercontinumm generation through photonic crystal fiber with As_2S_3 chalcogenide core. *J. Lightwave Techn.*, 2016; 34(23): 5423–5430. https://doi.org/10.1109/JLT.2016.2615044
15. Begum F., Namihira Y., Kaijage S.F., Kinjo T. Broadband supercontinuum spectrum generated highly nonlinear photonic crystal fiber applicable to medical and optical communication systems. *Jpn. J. Appl. Phys.*, 2011; 50(9R): 092502-092507. https://doi.org/10.1143/JJAP.50.092502
16. Begum F., Namihira Y. Design of supercontinuum generating photonic crystal fiber at 1.06, 1.31 and 1.55 μm wavelengths for medical imaging and optical transmission systems. *Natural Science*, 2011; 3(5): 401–407. https://doi.org/10.4236/ns.2011.35054
17. Zhu Z., Brown T.G. Full-vectorial finite-difference analysis of microstructured optical fibers. *Opt. Express*, 2002; 10(17): 853–864. https://doi.org/10.1364/OE.10.000853
18. Guo S., Wu F., Albin S., Tai H., Rogowski R.S. Loss and dispersion analysis of microstructured fibers by finite-difference method. *Opt. Express*, 2004; 12(15): 3341–3352. https://doi.org/10.1364/OPEX.12.003341
19. Begum F., Namihira Y., Razzak S.M.A., Zou N. Novel square photonic crystal fibers with ultra-flattened chromatic dispersion and low confinement losses. *IEICE Transaction on Electronics*, 2007; E90-C (3): 607–612. DOI: 10.1093/ietele/e90-c.3.607
20. Agrawal G. Nonlinear Fiber Optics. Academic Press (CA), 1995. 592 p. https://doi.org/10.1016/C2009-0-21165-2